Incorporating β-Turns and a Turn Mimetic out of Context in Loop 1 of the WW Domain Affords Cooperatively Folded β-Sheets

Ramesh Kaul, Angie R. Angeles, Marcus Jäger, Evan T. Powers, and Jeffery W. Kelly*

Contribution from the Department of Chemistry and The Skaggs Institute for Chemical Biology, The Scripps Research Institute, 10550 North Torrey Pines Road, BCC 506, La Jolla, California 92037

Received February 1, 2001

Abstract: To probe the conformational requirements of loop 1 in the Pin1 WW domain, the residues at the $i + 2$ and $i + 3$ positions of a β-turn within this loop were replaced by dPro-Gly and Asn-Gly, which are known to prefer the conformations required at the $i + 1$ and $i + 2$ positions of type II′ and type I′ β-turns. Conformational specificity or lack thereof was further examined by incorporating into the $i + 2$ and $i + 3$ positions a non-α-amino acid-based β-turn mimetic (4-(2′-aminoethyl)-6-dibenzofuran propionic acid residue, **1**), which was designed to replace the $i + 1$ and $i + 2$ positions of β-turns. All these Pin WW variants are monomeric and folded as discerned by analytical ultracentrifugation, NMR, and CD. They exhibit cooperative two-state transitions and display thermodynamic stability within 0.5 kcal/mol of the wild-type WW domain, demonstrating that the acquisition of native structure and stability does not require a specific sequence and, by extension, conformation within loop 1. However, it could be that these loop 1 mutations alter the kinetics of antiparallel β-sheet folding, which will be addressed by subsequent kinetic studies.

Introduction

Engineering β-sheet proteins to understand their stability and mechanism of folding is an area of considerable recent interest.[1] The general lessons learned from analysis of protein-based data, such as β-sheet propensities and preferences for interstrand residue pairings, have been valuable tools in these efforts.[2] It has become clear, however, that the roles of loops (or reverse turns) in β-sheet folding have to be defined separately for each individual system.[3] In some cases, they are essential for the nucleation and stability of β-sheets[4,5] while in others, they are simply flexible linkers between modules of secondary structure;[6] clearly, their role is context-dependent.[4] The issue of loop importance has usually been addressed in the context of either full proteins or minimal β-hairpin peptides.[3,4] A bridge between the complexity of the former systems and the simplicity of the latter are β-sheet mini-proteins. β-Sheet mini-proteins are ideal model systems for the study of β-sheet folding in general and the role of loops specifically.[7] Unlike full proteins, they are readily accessible by both routine solid-phase peptide synthesis and recombinant approaches, and unlike β-hairpin peptides (whose folding is only weakly cooperative[8]) they exhibit cooperative transitions between the folded and unfolded states that facilitate detailed kinetic and thermodynamic analysis.

In our continuing efforts to understand β-sheet folding, we have chosen to study β-sheet mini-proteins derived from WW domains, named after the two conserved tryptophan residues in this family of domains with over 200 members.[9] WW domains are structural motifs found in many multidomain proteins. They bind proline-rich ligands and are often involved in protein−protein interactions.[9] Here we examine the β-sheet mini-protein derived from the N-terminal WW domain (residues 6−39) of Pin1 (human rotamase or peptidyl-prolyl *cis*−*trans*

* Corresponding author. Voice: 858-784-9605. FAX: 858-784-9610. E-mail: jkelly@scripps.edu.

(1) EsPinosa, J. F.; Gellman, S. H. *Angew. Chem., Int. Ed. Engl.* **2000**, *39*, 2330−2333. Villegas, V.; Zurdo, J.; Filimonov, V. V.; Aviles. F. X.; Dobson, C. M.; Serrano, L. *Protein Sci.* **2000**, *9*, 1700−1708. Hamuro, Y.; Schneider, J. P.; DeGrado, W. F. *J. Am. Chem. Soc.* **1999**, *121*, 12200−12201. Ramirez-Alvarado, M.; Kortemme, T.; Blanco, F. J.; Serrano, L. *Bioorg. Med. Chem.* **1999**, *7*, 93−103. Lacroix, E.; Kortemme, T.; De La Paz, M. L.; Serrano, L. *Curr. Opin. Struct. Biol.* **1999**, *9*, 487−493. Lim, A.; Saderholm, M. J.; Makhov, A. M.; Kroll, M.; Yan, Y.; Perera, L.; Griffith, J. D.; Erickson, B. W. *Protein Sci.* **1998**, *7*, 1545−1554. Gellman, S. H. *Curr. Opin. Chem. Biol.* **1998**, *2*, 717−725. West, M. W.; Beasley, J. R.; Hecht, M. H. *Protein Eng.* **1997**, *10*, 38. DeGrado. W. F. *Science* **1997**, *278*, 80−81. Ilyina, E.; Roongta, V.; Mayo, K. *Biochemistry* **1997**, *36*, 5245−5250. Smith, C. K.; Regan, L. *Acc. Chem. Res.* **1997**, *30*, 153−161. Quinn, T. P.; Tweedy, N. B.; Williams, R. W.; Richardson, J. S.; Richardson, D. C. *Proc. Natl. Acad. Sci. U.S.A.* **1994**, *91*, 8747−8751. Yan, Y.; Erickson, B. W. *Protein Sci.* **1994**, *3*, 1069−1073. Hecht, M. H. *Proc. Natl. Acad. Sci. U.S.A* **1994**, *91*, 8729−8730. Pessi, A.; Bianchi, E.; Crameri, A.; Venturin, S.; Tramontano, A.; Sollazzo, M. *Nature* **1993**, *362*, 367−369.

(2) Minor, D. L., Jr.; Kim, P. S. *Nature* **1996**, *380*, 730−734. Wouters, M. A.; Curmi, P. M. *Proteins* **1995**, *22*, 119−131. Sibanda, B. L.; Thornton, J. M. *J. Mol. Biol.* **1993**, *229*, 428−447 and references therein. Gunasekharan, K.; Ramakrishnan, C.; Balaram, P. *Protein Eng.* **1997**, *10*, 1131−1141. Smith, C. K.; Regan, L. *Science* **1995**, *270*, 980−982. Hutchinson, E. G.; Thornton, J. M. *Protein Sci.* **1994**, *3*, 2207−2216. Minor, D. L., Jr.; Kim, P. S. *Nature* **1994**, *371*, 264−267. Minor, D. L., Jr.; Kim, P. S. *Nature* **1994**, *367*, 660−663., Regan, L. *Curr. Biol.* **1994**, *4*, 656−658.

(3) Gruebele, M.; Wolynes, P. G. *Nat. Struct. Biol.* **1998**, *5*, 662−665.

(4) Takano, K.; Yamagata, Y.; Yutani, K. *Biochemistry*, **2000**, *39*, 8655−8665. Gu, H.; Kim, D.; Baker, D. *J. Mol. Biol.* **1997**, *274*, 588−596. Zhou, H. X.; Hoess, R. H.; DeGrado, W. F. *Nat. Struct. Biol.* **1996**, *3*, 446−451. Ybe, J. A.; Hecht, M. H. *Protein Sci.* **1996**, 5, 814−824.

(5) Garrett, J. B.; Mullins, L. S.; Raushel, F. M. *Protein Sci.* **1996**, *5*, 204−211. Helms, L. R.; Wetzel, R. *Protein Sci.* **1995**, *4*, 2073−2081. Hynes, T. R.; Kautz, R. A.; Goodman, M. A.; Gill, J. F.; Fox, R. O. *Nature* **1989**, *339*, 73−76.

(6) Viguera, A. R.; Blanco, F. J.; Serrano, L. *J. Mol. Biol.* **1995**, *247*, 670−681.

(7) Kortemme, T.; Ramirez-Alvarado, M.; Serrano, L. *Science* **1998**, *281*, 253−256. Schenck, H. L.; Gellman, S. H. *J. Am. Chem. Soc.* **1998**, *120*, 4869−4870.

(8) Sharman, G. J.; Searle, M. S. *J. Am. Chem. Soc.* **1998**, *120*, 5291−5300. Griffith-Jones, S. R.; Searle, M. S. *J. Am. Chem. Soc.* **2000**, *122*, 8350−8356.

(9) Sudol, M.; Hunter, T. *Cell* **2000**, *103*, 1001−1004. Sudol, M. *Prog. Biophys. Mol. Biol.* **1996**, *65*, 113−132. Staub, O.; Rotin, D. *Structure* **1996**, *4*, 495−499. Macias, M. J.; Hyvonen, M.; Baraldi, E.; Schultz, J.; Sudol, M. *Nature* **1996**, *382*, 646−649.

10.1021/ja0102890 CCC: $20.00
Published on Web 05/12/2001

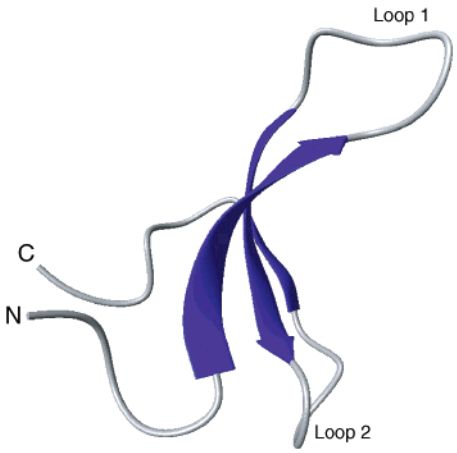

Figure 1. Ribbon diagram of the polypeptide backbone of the isolated WW domain from Pin1. The figure was prepared using MOLMOL[29] based on the coordinates from the X-ray structure of Pin.[11]

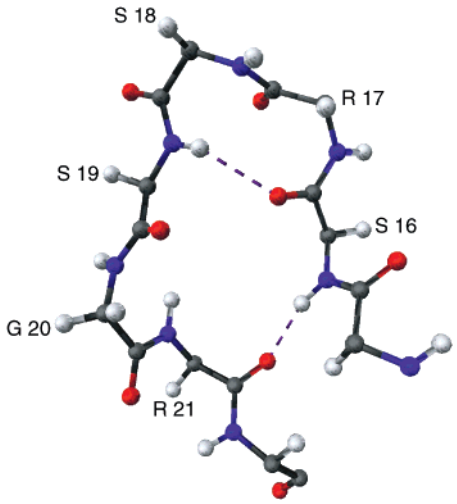

Figure 2. Ball-and-stick representation of the residues forming loop 1 and their conformation in the Pin1 WW domain. This Figure was designed using MOLMOL[24] and does not depict the entire side chain.

isomerase), a mitosis cell cycle regulator.[10] The crystal structure of Pin1 has been solved to 1.35 Å resolution.[11] The portion of the structure corresponding to its N-terminal WW domain is shown in ribbon diagram format in Figure 1. The WW domain folds into a three-stranded antiparallel β-sheet conformation with two loops, one consisting of six residues (loop 1, Ser16-Arg 21), and a π loop consisting of four residues (loop 2, His27-Asn30).[12] The wild type WW domain of Pin1 is independently folded, is stable ($\Delta G_{\text{unfolding}} = 3.3$ kcal/mol), and exhibits a sigmoidal unfolding curve upon thermal and chaotropic denaturation (vide infra). With this in mind, we set out to explore the possibility of reengineering the loop segments to determine their roles in its folding. However, it was evident from the crystal structure of the full protein that loop 2 is in proximity to the other domain of Pin1 (the PPIase domain), whereas loop 1 is solvent-exposed. Because packing may influence the conformation of loop 2 observed in the crystal structure, we chose to focus our efforts on loop 1. Figure 2 shows the conformation of the residues in and around loop1, while Table 1 lists the

Table 1: Backbone Dihedral Angles (ϕ, ψ) of Residues S16−R21 Forming Loop 1

residue	ϕ (deg)	Ψ (deg)
S 16	−68.59	−140.22
R 17	−65.22	139.93
S 18	62.92	26.81
S 19	−148.64	173.18
G 20	−107.77	9.08
R 21	−74.80	114.20

corresponding ϕ, ψ angles. Residues S16 through S19 form a type II β-turn centered around R17 ($i + 1$) and S18 ($i + 2$) within the loop. This is apparent both from the ϕ, ψ angles (compare to the expected values of $\phi_{i+1} = -60°$, $\psi_{i+1} = 120°$ and $\phi_{i+2} = 80°$, $\psi_{i+2} = 0°$) and from the hydrogen bond between the CO of S16 (i) and the NH of S19 ($i + 3$). Following the $i + 1$ and $i + 2$ residues of this type II β-turn are S19 in an extended (ϵ) conformation, G20 in a conformation that does not fall into any of the standard ϕ, ψ regions, and R21 which resumes the sheet. These last residues confer upon the loop an overall conformation that is not commonly observed in the loops of other proteins. To test the necessity or lack thereof of this conformation and its role in WW stability, we sought to replace the $i + 2$ and $i + 3$ residues of the β-turn (S18 and S19) with dipeptide sequences that have known preferences to adopt dissimilar conformations, that is, conformations typically adopted at the $i + 1$ and $i + 2$ positions of a β-turn. We expected such substitutions to have one of two possible effects on the structure and stability. If the loop requires a defined conformation, then the substitutions should be very disruptive to the structure, and the mutant mini-proteins should be much less stable than the wild type, if they are folded at all. If a specific loop conformation is not required for β-sheet structure, then it ought to be able to accommodate the substitutions without undue strain, and the mutants should have stabilities comparable to those of the wild type. The dipeptide residues chosen for this substitution experiment were dPro-Gly and Asn-Gly. These are well-known to adopt the conformations required by the $i + 1$ and $i + 2$ residues of type II′ and type I′ β-turn conformations, respectively, and they have both been used extensively in the design of β-hairpin peptides.[13,14]

In addition, the conformational requirements of loop1 could also be evaluated by incorporating one of the non-peptide scaffolds that have been used to induce β-hairpins in short peptides.[15] We have chosen to work with the 4-(2′-aminoethyl)-6-dibenzofuranpropionic acid residue (**1**), designed to replace the $i + 1$ and $i + 2$ residues of a β-turn. This β-turn mimic has been shown by our group to promote β-hairpin formation in short peptides.[16] It has also been incorporated in place of the *i*

(10) Lu, K. P.; Hanes, S. D.; Hunter, T. *Nature* **1996**, *380*, 544−547. Lu, P. J.; Zhou, X. Z.; Lu, K. P. *Science* **1999**, *283*, 1325.

(11) Ranganathan, R.; Lu, K. P.; Hunter, T.; Noel, J. P. *Cell* **1997**, *89*, 875−886.

(12) We have defined the turn as proposed in Kabsch, W.; Sander, C. *Biopolymers* **1983**, *22*, 2577−2637.

(13) Stangers, H. E.; Gellman, S. H. *J. Am. Chem. Soc.* **1998**, *120*, 4236−4237. Blanco, F.; Ramirez-Alvarado, M.; Serrano, L. *Curr. Opin. Struct. Biol.* **1998**, *8*, 107−111. Karle, I. L.; Awasthi, S. K.; Balaram, P. *Proc. Natl. Acad. Sci. U.S.A.* **1996**, *93*, 8189−8193.

(14) Maynard, A. J.; Sharman, G. J.; Searle, M. S. *J. Am. Chem. Soc.* **1998**, *120*, 1996−2007. De Alba, E.; Jimenez, M. A.; Rico, M.; Nieto, J. L. *J. Am. Chem. Soc.* **1997**, *119*, 175−183. Haque, T. S.; Gellman, S. H. *J. Am. Chem. Soc.* **1997**, *119*, 2303−2304.

(15) Nowick, J. S.; Chung, D. M.; Maitra, K.; Maitra, S.; Stigers, K. D.; Sun, Y. *J. Am. Chem. Soc.* **2000**, *122*, 7654−7661. Stigers, K. D.; Soth, M. J.; Nowick, J. S. *Curr. Opin. Chem. Biol.* **1999**, *3*, 714−723. Junquera, E.; Nowick, J. S. *J. Org. Chem.* **1999**, *64*, 2527−2531. Kemp, D. S.; Li, Z. Q. *Tetrahedron Lett.* **1995**, *36*, 4179−4180. Nesloney, C. L.; Kelly, J. W. *Bioorg. Med. Chem.* **1996**, *4*, 739−766. Tsang, K. Y.; Diaz, H.; Graciani, N.; Kelly, J. W. *J. Am. Chem. Soc.* **1994**, *116*, 3988−4005. Baca, M.; Alewood, P. F.; Kent, S. B. H. *Protein Sci.* **1993**, *2*, 1085−1091.

(16) Diaz, H.; EsPina, J. R.; Kelly, J. W. *J. Am. Chem. Soc.* **1992**, *114*, 8316−8318. Diaz, H.; Tsang, K. Y.; Choo, D.; EsPina, J. R.; Kelly, J. W. *J. Am. Chem. Soc.* **1993**, *115*, 3790−3791. Tsang, K. Y.; Diaz, H.; Graciani, N.; Kelly, J. W. *J. Am. Chem. Soc.* **1994**, *116*, 3988−4005.

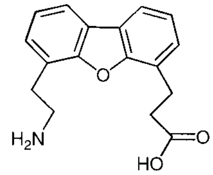

1

+ 1 and *i* + 2 residues in the turn region of two small proteins where it was found to be compatible with *β*-sheet structure, although the folds were slightly destabilized relative to the α-amino acid based sequence.[17] In peptide *β*-hairpins **1** functions optimally as a *β*-turn inducer when flanked by hydrophobic residues. Here, it is flanked by Arg and Gly residues, hence it is not clear whether the dibenzofuran ring is oriented perpendicular to the *β*-sheet interacting with the N-propyl substructure of the Arg residue or whether it is in an extended conformation.[16] Either of these low energy conformations should impart strong conformational constraints on the loop, and thus suit the requirements of this study. Similar to the dPro-Gly and Asn-Gly substitutions, the constraints introduced by the dibenzofuran turn mimic into loop 1 should disrupt the structure if the loop's conformational requirements are rigid.

Results

The wild-type WW domain was made recombinantly using the GST-Pin(6−39) fusion protein as described in the Experimental Section, while the three mutants discussed above were chemically synthesized by a solid-phase peptide synthesis strategy using Fmoc chemistry. All of their sequences are shown below. The recombinant Pin WW domain has two additional residues (Gly and Ser) at the N-terminus which resulted from proteolytic cleavage of the GST-Pin(6−39) linker peptide. The *β*-turn mimic (**1**) was synthesized using methods developed by our group.[18] Its incorporation in the protein was carried out by manual manipulation of the resin bound peptide as described in the Experimental Section.

```
              6                                                   39
Pin WT---G S K L P P G W E K R M S R  S S  G R V Y Y F N H I T N A S Q W E R P S G
Pin NG --------K L P P G W E K R M S R N G  G R V Y Y F N H I T N A S Q W E R P S G
Pin dPG-------K L P P G W E K R M S R dPG  G R V Y Y F N H I T N A S Q W E R P S G
Pin DBF-------K L P P G W E K R M S R  1   G R V Y Y F N H I T N A S Q W E R P S G
```

The thermodynamic analysis of these mini-proteins requires that they be both monomeric and stable. The former issue was addressed by sedimentation equilibrium analytical ultracentrifugation (AUC). The AUC data were obtained for each mini-protein (40 *μ*M) in phosphate buffer at pH 7.0. Each set of data was fit to a single ideal species model (see Supporting Information); the molecular weights obtained from the fits were comparable to the theoretical masses of the monomers in every case. This, together with the small, randomly distributed residuals[19] indicates that all of the mini-proteins were monomeric in aqueous solution, including the wild-type sequence. In addition, the tendency or lack thereof of Pin WT to associate at higher concentrations was assessed by variable concentration CD spectroscopy. The CD spectrum of Pin WT does not change over the concentration range from 40 to 200 *μ*M, indicating that it remains monomeric over this range. The issue of whether these domains are folded was addressed by CD and NMR spectroscopy. The far-UV CD spectra measured at 4 °C of the three Pin mutants in comparison to the WT domain are shown in Figure 3. Each of these has a prominent positive band at 227 nm, most likely attributable to aromatic contributions to the far-UV CD spectrum (as was shown previously using W to F mutants of the hYap WW domain[20a,b]). While this does not resemble the commonly accepted CD spectrum of *β*-sheets, which has a minimum at 215−218 nm, this feature seems to be common to WW domains, since it has been observed in the hYap WW domain as well.[20a] The amide/aromatic and upfield regions of the NMR spectra of the three Pin mutants were recorded and compared to that of the wild type at 4 °C (Figure 4). In all four cases, the signals are well dispersed, with a number of peaks appearing downfield of 8.5 ppm, similar to the hYap WW domain NMR spectrum.[20a] The CD and NMR spectra show that Pin-NG and Pin-DBF are folded, and that their fold is similar to that of the wild-type mini-protein (the NMR structure of which has been recently determined by our group in the absence of the ligand,[21] providing further evidence for the lack

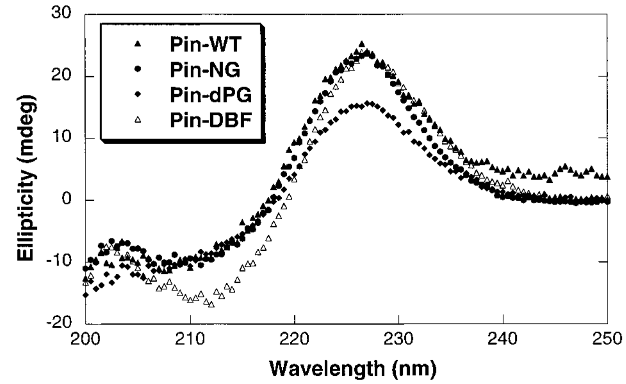

Figure 3. Far-UV CD spectra of 40 *μ*M solutions of the WW domains in 10 mM sodium phosphate buffer (pH 7.0) at 4 °C.

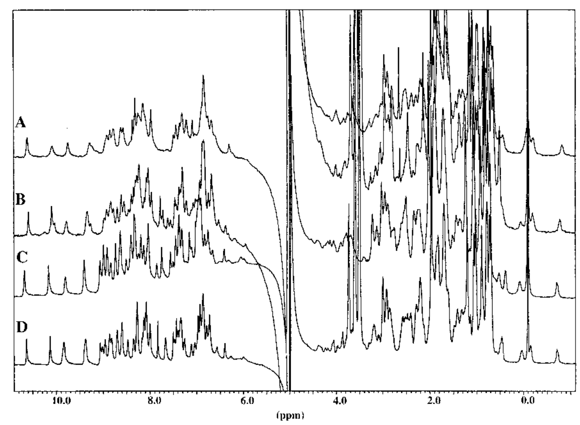

Figure 4. ^{1}H NMR spectra of 500 *μ*M solutions of the WW domains (A) Pin-DBF, (B) Pin-dPG, (C) Pin-NG, and (D) Pin-WT. Spectra were acquired at 600 MHz in 90% H_2O buffered with 50 mM sodium phosphate (pH 6.2), 10% D_2O at 5 °C.

(17) Odaert, B.; Jean, F.; Boutillon, C.; Buisine, E.; Melnyk, O.; Tartar, A.; Lippens, G. *Protein Sci.* **1999**, *8*, 2773−2783. Jean, F.; Buisine, E.; Melnyk, O.; Drobecq, H.; Odaert, B.; Hughues, M.; Lippens, G.; Tartar, A. *J. Am. Chem. Soc.* **1998**, *120*, 6076−6083.

(18) Bekele, H.; Nesloney, C. L.; McWilliams, K. W.; Zacharias, N. M.; Niki, M.; Chitnumsub, P.; Kelly, J. W. *J. Org. Chem.* **1997**, *62*, 2259−2262.

(19) The residuals are the difference between the experimental data and the theoretical fit to the data.

(20) (a) Koepf, E. K.; Petrassi, H. M.; Sudol, M.; Kelly, J. W. *Protein Sci.* **1999**, *8*, 841−853. (b) Koepf, E. K.; Petrassi, H. M.; Ratnaswamy, G.; Huff, M. E.; Sudol, M.; Kelly, J. W. *Biochemistry*. **1999**, *38*, 14338−14351. (c) Crane, J. C.; Koepf, E. K.; Kelly, J. W.; Gruebele, M. *J. Mol. Biol.* **2000**, *298*, 283−292.

(21) Kowalski, J.; Liu, K.; Kelly, J. W. Manuscript in preparation.

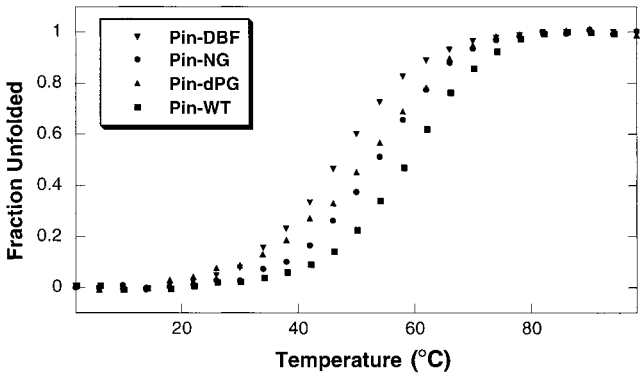

Figure 5. Thermal denaturation profiles in terms of fraction unfolded for the WW domains as monitored by far-UV CD at 227 nm. The protein concentration was 40 μM in 10 mM sodium phosphate buffer (pH 7.0), and the samples were heated from 2 to 98 °C with 10 min equilibration time at each new temperature.

Table 2: Thermodynamic Parameters for the Equilibrium Unfolding of the Wild-Type Pin1 WW Domain and Its Variants

	T_m (°C)		$\Delta G_{unfolding}$ (kcal/mol) at 4 °C from GuHCl denaturation	
protein	far UV−CD	near UV−CD	far UV−CD	fluorescence
Pin-WT	58.0 ± 0.2	−	3.3 ± 0.1	3.4 ± 0.2
Pin-NG	54.4 ± 0.2	−	2.8 ± 0.1	2.8 ± 0.2
Pin-dPG	54.8 ± 0.6	−	3.5 ± 0.2	3.7 ± 0.1
Pin-DBF	48.2 ± 0.3	48.1 ± 0.2	3.6 ± 0.1	−

of assembly at higher concentration). For Pin-dPG, the presence of additional weak resonances between 9 and 10.5 ppm may result from a small population of an alternatively folded WW domain, possibly due to *cis*−*trans*-proline isomerization. Otherwise, its CD and NMR spectra indicate that the dominant species has the same fold as the Pin-WT.

A variety of spectroscopic methods (far- and near-UV CD, fluorescence) were used to characterize the folding thermodynamics of each Pin WW domain variant. In all four cases, thermal unfolding was measured through the temperature range of 2−98 °C by monitoring the CD ellipticity at 227 nm. The thermal denaturation profiles in terms of the fraction unfolded are shown in Figure 5, and the T_m's obtained by fitting the data to a two-state model (see Experimental Section) are recorded in Table 2. The CD spectra measured at 2 °C before heating and after cooling were identical except for a slight loss in ellipticity, as has been observed in studies of the hYap WW domain (data not shown).[20a] In addition to thermal unfolding, GuHCl-induced unfolding (4 °C) of all sequences was monitored by CD ellipticity at 227 nm. The chaotropic denaturation profiles, in terms of the fraction unfolded, are shown in Figure 6. These data were analyzed as described in the Experimental Section, and the resulting free energies of unfolding at 4 °C are listed in Table 2.

Since these mini-proteins have conserved tryptophan residues, fluorescence emission spectroscopy can be used to monitor changes in their tertiary structure upon unfolding, complementing the changes in secondary and tertiary structure monitored by CD. The emission maxima of tryptophan residues in proteins red shift as a protein is unfolded because the polarity of their environment increases. The intensity can either increase or decrease as quenching can be less or more efficient when tryptophan is solvent-exposed. The fluorescence emission spectra of native Pin-WT, Pin-NG, and Pin-dPG were similar to each other and to that of the hYap WW domain[20a] with an emission maximum at 342 nm (excitation at 295 nm, see inset to Figure 7). The GuHCl-induced denaturation curves at 4 °C for Pin-WT, Pin-NG, and Pin-dPG were measured by monitoring the decrease in fluorescence intensity at 342 nm. These are shown in Figure 7, and as with the data in Figure 6, they were analyzed as described in the Experimental Section, and the resulting ΔG values at 4 °C are listed in Table 2.

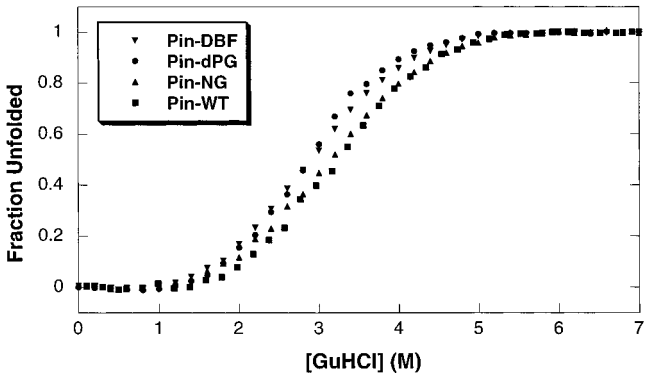

Figure 6. GuHCl-induced denaturation curves at 4 °C showing fraction unfolded for the WW domains (5 μM) in 10 mM sodium phosphate buffer (pH 7.0) as monitored by far-UV CD at 227 nm.

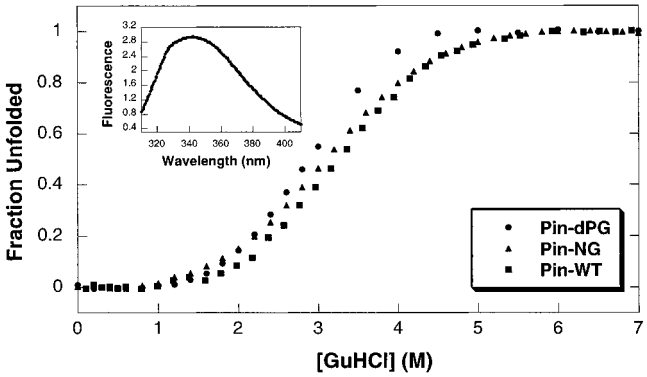

Figure 7. GuHCl-induced denturation profiles at 4 °C for wild-type WW and variants thereof (2 μM) in 10 mM sodium phosphate buffer (pH 7.0) monitored by fluorescence intensity at 342 nm. A representative emission spectrum of the WW domain and the mutants at 4 °C (excitation at 295 nm) is shown in the inset.

The Pin-DBF mutant could not be studied by fluorescence because the dibenzofuran substructure contributed to the spectrum and overwhelmed the signal from the tryptophans (data not shown). Therefore, instead of using fluorescence, we used near-UV CD to monitor changes in tertiary structure. The near-UV CD of Pin-DBF showed a positive peak at 269 nm (see the inset to Figure 8) similar to that of the WT (data not shown). This wavelength was used to monitor the thermal denaturation under conditions analogous to those used for far-UV CD (Figure 8). The data were fit as before to eq 1, and the T_m is listed in Table 2.

Discussion

The unfolding transitions for Pin-dPG, Pin-NG and Pin-DBF are rather broad, as expected because such a short sequence should have a small ΔS and ΔC_p of unfolding.[22] Nevertheless, the clearly sigmoidal shape of their thermal and chaotropic denaturation curves indicates substantial cooperativity very similar to that exhibited by the wild-type Pin domain. There are also strong indications from the plots in Figure 9 that these transitions involve only a native state and an unfolded state.

(22) Alexander, P.; Fahnestock, S.; Lee, T.; Orban, J.; Bryan, P. *Biochemistry* **1992**, *31*, 3597−3603.

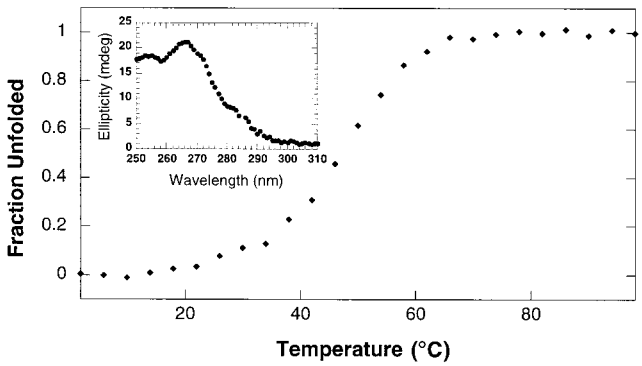

Figure 8. Thermal denaturation profile showing the fraction of Pin-DBF unfolded as a function of temperature monitored by near-UV CD. The protein sample (150 μM) in 10 mM sodium phosphate buffer (pH 7.0) was heated from 2 to 98 °C with a 10 min equilibration time at each new temperature. A near-UV CD scan of a 150 μM solution of Pin-DBF in 10 mM sodium phosphate buffer at 2 °C is shown in the inset.

Figure 9a,b,c shows the superimposition of the chaotrope-induced denaturation as monitored by far-UV CD and fluorescence for the wild type (Pin-WT), Pin-dPG and Pin-NG mutants, respectively. A similar plot is shown in Figure 9d for the thermal unfolding of the Pin-DBF mutant with the far- and near-UV CD data. The superimposition of unfolding curves obtained from different spectroscopic methods such as far-UV CD and fluorescence or far- and near-UV CD shows that the unfolding of the secondary and tertiary structure is coincident in the wild type and each variant. Since there are no detectable intermediates in which secondary structure is retained while tertiary structure is lost (or vice versa), the unfolding transition is most likely two-state. Kinetic studies on the Pin-WT confirms this expectation.[23]

Given that the unfolding of all of the Pin WW variants is both cooperative and apparently two-state, the thermodynamic data in Table 2 can now be interpreted in terms of the conformational requirements of loop 1. All of the mutants exhibit resistance to thermal denaturation comparable to the wild-type Pin WW domain. The T_m values range over only 10 °C, from 58 °C for the wild type to 48°C for the Pin-DBF mutant, with the dPG and NG mutants falling in between. The stabilities of the mutants with respect to chaotrope denaturation are within 0.5 kcal/mol of the wild type, with the DBF and dPG mutants exhibiting slightly increased stability. As was noted above, the introduction of the dipeptides dPro-Gly and Asn-Gly into positions 18 and 19 should have resulted in dramatically altered stability of the mini-protein if the loop had specific conformational requirements; however, this was not observed. The conformational preferences introduced into loop 1 by dPro-Gly and Asn-Gly were easily accommodated, without major disruptions in stability or structure in comparison to that in the wild-type protein, as determined by NMR. The introduction of the non-peptidic turn template **1** should be an even stronger test of the conformational requirements in and around the loop. Pin-DBF is in fact the least resistant variant to thermal denaturation, its T_m being significantly (10 °C) less than the WT. However, its stability measured in chaotropes by the linear extrapolation method is greater than that of the rest of the variants. This again shows that the loop's conformational requirements are flexible enough to accommodate this $(i + 1)-(i + 2)$ β-turn dipeptide mimetic in place of the $i + 2$ and $i + 3$ positions of the β-turn that exists within the loop 1, although at the expense of thermal stability.

In conclusion, the Pin1 WW domain is independently folded and stable with a wide variety of sequences incorporated into loop 1. This demonstrates that thermodynamic stability does not require a specific loop 1 sequence and therefore a specific conformation. However, it does not mean that the loop sequence is not important for folding; these variants could exhibit dramatically altered folding rates, implying its importance in transition-state structure. A ϕ value analysis will be carried out on these variants to address this possibility experimentally.[20c]

Experimental Section

The wild-type WW domain was made recombinantly. The gene sequence encoding residues 6−39 was amplified by PCR starting from a plasmid encoding the full-length Pin1-rotamase (vector kindly provided by M. Verdecia and Dr. J. Noel, The Salk Institute, La Jolla, CA) and cloned into the commercially available expression vector pGEX-2T (Pharmacia). The GST-fusion protein thus obtained was then expressed and purified as described previously for the hYap WW domain.[20a,b] Typical yields were about 2 mg/L culture. The purified WW domain was dialyzed against 10 mM sodium phosphate buffer (pH 7.0) and stored at 4 °C until used. Protein identity and homogeneity was analyzed by electrospray ionization mass spectrometry (ESI-MS; expected mass = 4167.6; observed = 4167.2) as summarized below and reverse phase HPLC, respectively. The WW mutants studied were chemically synthesized using an ABI 433A peptide synthesizer (Applied Biosystems Inc., Foster City, CA). Reagents used for peptide synthesis were purchased from Fisher, Aldrich, or Applied Biosystems Inc, except that Fmoc-protected amino acids and Wang acid resin were acquired from Novabiochem (Calbiochem-Novabiochem Corp., La Jolla, CA). All materials were used without further purification. The dibenzofuran-based amino acid template, 4-(2′-aminoethyl)-6-dibenzofuranpropionic acid (**1**) was synthesized as described previously.[17] High performance liquid chromatography (HPLC) was carried out using a Waters 600E multisolvent delivery system (Waters Corporation, Milford, MA) equipped with either a Waters 2487 dual absorbance detector or a Waters 486 tunable absorbance detector. VYDAC C_{18} protein and peptide reverse phase columns were used with flow rates of 1 and 10 mL/min for analytical and preparative HPLC, respectively. Linear gradients of two solvent mixtures, solvent A (95% water, 4.8% acetonitrile, 0.2%TFA) and solvent B (95% acetonitrile, 4.8% water, 0.2%TFA) were used for analysis and purification. Typically, chromatography was monitored by absorbance at 214 and 280 nm. Thermodynamic studies were carried out in 10 mM sodium phosphate buffer (pH 7.0). Concentrations were determined spectrophotometrically using ϵ_{280} = 13940 M^{-1} cm^{-1} (for Pin-NG, Pin-dPG, Pin-WT) as calculated using the method of Edelhoch.[24] For Pin-DBF the extinction coefficients of the protein and DBF[25] were added to yield ϵ_{280} = 31737 M^{-1} cm^{-1}.

Peptide Synthesis. The Pin mutants were synthesized by solid-phase peptide synthesis utilizing Fmoc chemistry. The side chain-protected amino acids used were Fmoc-Arg(Pbf)-OH, Fmoc-Asp(*tert*-Butyl)-OH, Fmoc-Asn(Trt)-OH, Fmoc-His(Trt)-OH, Fmoc-Gln(Trt)-OH, Fmoc-Glu(*tert*-Butyl)-OH, Fmoc-Lys(t-Boc)-OH, Fmoc-Ser(*tert*-Butyl)-OH, Fmoc-Thr(*tert*-Butyl)-OH, Fmoc-Trp(t-Boc)-OH, and Fmoc-Tyr(*tert*-Butyl)-OH. The synthesis was initiated using preloaded Fmoc-Gly on a Wang resin (0.1 mmol/g), and the chain extension was accomplished on the automated synthesizer using the standard Fmoc-based FastMoc coupling chemistry provided by the system's software. Briefly, the coupling reactions were carried out in *N*-methylpyrrolidone (NMP) using 10 equiv of amino acid and the activating agents (2-(1H-benzotriazol-1-yl)-1,1,3,3-tetramethyluronium hexafluorophosphate (10 equiv) and 1-hydroxybenzotriazole (10 equiv) in the presence of diisopropylethylamine (10 equiv). The N-terminal Fmoc deprotection was achieved using 20% piperidine in DMF for 30 min. The template

(23) Jager, M.; Nguyen, H.; Crane, J.; Kelly, J. W.; Gruebele, M. Manuscript submitted.

(24) Edelhoch, H. *Biochemistry*. **1967**, *6*, 1948−1954.

(25) Bekele, H. Ph.D. Dissertation, Texas A & M University, August, 1999.

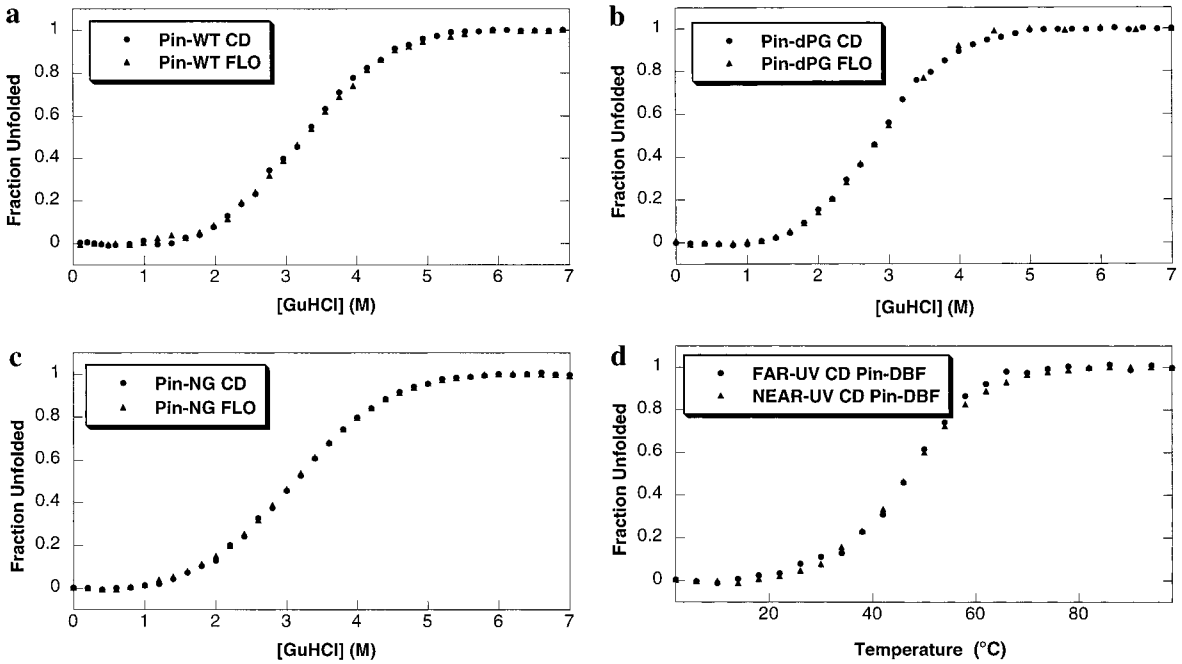

Figure 9. Denaturation profiles for WW and its variants demonstrating the presence of only a native and an unfolded state as indicated by superimposition of curves derived from different spectroscopic techniques. Panels a, b, and c show that the chaotrope-induced unfolding transitions are superimposable when monitored by far-UV CD and fluorescence (FLO) for wild type, Pin-dPG, and Pin-NG, respectively. Panel d shows that the thermal unfolding transitions as monitored by far- and near-UV CD are indistinguishable for Pin-DBF.

1 (1.2 equiv) was incorporated manually using 1.2 equiv of the activating agents HBTU/HOBT in DMF (2 mL) in the presence of 2.2 equiv of diisopropylethylamine (2 M in NMP). The coupling was carried out for 24 h before loading the resin back on the synthesizer for further extension of the peptide chain. The final deprotection and cleavage was achieved by shaking the resin-bound peptide (100 mg) with the cleavage mixture of TFA (2 mL), water (100 μL), thioanisole (100 μL), *m*-cresol (100 μL), and ethanedithiol (50 μL) for 2 h.[26] The resin was filtered off, and the filtrate was forced through a frit into cold *tert*-butylmethyl ether, causing the polypeptide to precipitate. The precipitate was centrifuged and washed several times with *tert*-butylmethyl ether. The dried solid was dissolved in water and then loaded onto a preparative HPLC for purification using a linear gradient of 20−80% B. The HPLC fractions were collected and analyzed by ESI-MS to confirm the products. A brief summary of this characterization is shown below:

polypeptide	expected mass	observed mass
Pin-NG	4020.5	4020.8
Pin-dPG	4003.5	4003.0
Pin-DBF	4114.6	4114.0

Acetonitrile and traces of TFA were removed by rotary evaporation and the aqueous solutions were lyophilized. The peptides were refolded by dissolving the lyophilized powder in 10 mM sodium phosphate buffer (pH 7.0) before proceeding with the thermodynamic studies.

CD Studies. CD measurements were made on an AVIV model 202SF stopped flow circular dichroism spectrometer equipped with a Peltier temperature-controlled cell holder using a 0.1 cm path length Suprasil quartz cell (Hellma, Forest Hills, New York). Far-UV CD spectra were recorded using 300 μL of a 40 μM solution of the WW domains in 10 mM phosphate buffer (pH 7.0). Thermal unfolding experiments were monitored at 227 nm over a temperature range of 2−98 °C with 10 min thermal equilibration at each 4 °C temperature step. Signals were averaged for 30 s. Identical parameters were used for the near-UV CD thermal denaturation curve carried out for the Pin-DBF mutant, except the 269 nm wavelength was monitored, the protein concentration was 150 μM, and a 1.0 cm path length was used. The thermal denaturation profiles were analyzed by a nonlinear least-squares fit, assuming the two-state model described by eq 1[27] and that $\Delta C_p = 0$.

$$Y = \frac{(y_n + m_n T) + (y_d + m_d T)\exp\left[\frac{\Delta H_m}{R}\left(\frac{1}{T_m} - \frac{1}{T}\right)\right]}{\left[1 + \exp\left[\frac{\Delta H_m}{R}\left(\frac{1}{T_m} - \frac{1}{T}\right)\right]\right]} \quad (1)$$

where Y is the observed ellipticity, ΔH_m is the enthalpy at the unfolding transition, T_m is the melting temperature, T is the temperature in Kelvin, and R is the universal gas constant. The parameters y_n and y_d refer to the y-intercepts of the native and the denatured baselines, respectively, while m_n and m_d are the slopes of the baselines (baselines were determined from the global fit). All experiments were performed in 10 mM sodium phosphate buffer at pH 7.0.

Guanidinium hydrochloride (GuHCl) denaturation was accomplished using the automated titrator accessory on the Aviv instrument model 202SF. Two solutions were prepared. The first being 5 μM protein in 10 mM phosphate buffer, and the second 5 μM protein and 7.0 M GuHCl in 10 mM phosphate buffer. The second solution was added to the first in steps such that the denaturant concentration of the mixture increased by 0.2 M/step while the protein concentration remained fixed. The equilibration time was fixed to 10 min for each addition with constant stirring. The data were collected at 227 nm with a 30 s averaging time. The denaturation curves were analyzed, assuming two-state behavior using eq 2:[27]

$$\Delta G = -RT \ln\left[\frac{(y_f - y)}{(y - y_u)}\right] \quad (2)$$

where ΔG is the free energy of unfolding at a given denaturant concentration, R is the gas constant, T is absolute temperature, and y_f and y_u are the ellipticities of the folded and unfolded states, respectively. Values of y_f and y_u in the transition region are obtained independently

(26) King, D. S.; Fields, C. G.; Fields, G. B. *Int. J. Pept. Protein Res.* **1990**, *36*, 255−266.

(27) Liskin, S.; Robertson, A. D. *Protein Sci.* **1993**, *2*, 2037−2049. Pace, C. N.; Scholtz, J. M. *Protein Struct.* (Creighton, T. E., Ed.) **1997**, 299−321.

by separate linear fits of the pre- and posttransition regions. The ΔG of unfolding is thus determined at a number of denaturant concentrations in the transition region, and the ΔG in the absence of denaturant is determined by linear extrapolation back to 0 M GuHCl.

Fluorescence. Fluorescence measurements were carried out on a AVIV model ATF105 automated differential/ratio spectrofluorometer. Emission spectra were recorded from 310 to 410 nm in 1 nm steps with excitation at 295 nm using a 1 × 0.6 cm cuvette. GuHCl denaturation experiments were conducted at 4 °C using the automated titrator accessory on the AVIV model ATF105 as described for the CD-monitored denaturation except that the protein concentration employed was 2 μM. Measurements were monitored at the maximum tryptophan emission at 342 nm. The denaturant was added in concentration steps of 0.2 M with an equilibration time of 10 min. The data were fitted to a two-state model using eq 2[27] as above.

^{1}H NMR Studies. The aqueous WW domain samples were analyzed by ^{1}H NMR using data recorded on a Bruker AMX 600 MHz spectrometer. The spectra were acquired at a spectral width of 9000 Hz at an operating frequency of 600 MHz using 800 points at 5 °C. Spectra were referenced to the methyl proton resonances of the internal standard 3-(trimethylsilyl) propionate-2,2,3,3-d_4 (Aldrich, Milwaukee, WI), which were assigned a chemical shift of 0.0 ppm. Sample concentrations of 500 μM in 10 mM sodium phosphate buffer at pH 7.0 (10% D_2O) was employed. Water suppression was achieved using the Watergate pulse sequence.[28] The data were processed using XWIN NMR software version 6.0 (Bruker) using a line-broadening parameter of 5 Hz.

(28) Piotto, M.; Saudek, V.; Skelnar, V. *J. Biomol. NMR* **1992**, *2*, 661−665.

(29) Koradi, R.; Billeter, M.; Wuthrich, K. *J. Mol. Graphics* **1996**, *14*, 51−55.

Analytical Ultracentrifugation. The monomeric nature of the samples was confirmed by sedimentation equilibrium measurements carried out employing a temperature-controlled Beckman XL-I Analytical Ultracentrifuge equipped with an An-60 Ti rotor and a photoelectric scanner (Beckman Instrument Inc., Palo Alto, CA). Protein samples (40 μM, 140 μL) in 10 mM sodium phosphate buffer (pH 7.0) were loaded in a double sector cell equipped with a 12 mm Epon centerpiece and a sapphire optical window. The reference compartment was loaded with a 10 mM sodium phosphate buffer (140 μL). The data were monitored at 280 nm employing a rotor speed of 30000 to 40000 at 20 °C and analyzed by a nonlinear squares approach using Origin software (Microcal Software Inc., Northampton, MA). The data were fitted to a single ideal species as described previously.[20a,b]

Acknowledgment. We gratefully acknowledge financial support from NIH (GM 51105), The Skaggs Institute of Chemical Biology, The Lita Annenberg Hazen Foundation, and The Hereditary Disease Foundation. M.J. thanks The Deutsche Forschungsgemeinschaft (DFG) for a postdoctoral fellowship. We thank Dr. Jennifer Kowalski for recording the NMR spectra of the WW domains, Songpon Deechongkit and H. Michael Petrassi for the analytical ultracentrifugation experiments, and Dr. Kai Liu for the MOLMOL figures. We also thank Dr. Xin Xiang for helpful discussions.

Supporting Information Available: Analytical ultracentrifugation data for all WW domains demonstrating their monomeric nature (PDF). This material is available free of charge via the Internet at http://pubs.acs.org.

JA0102890